THE MFS-SVD METHOD FOR THE LAPLACE EQUATION IN THREE DIMENSIONS*

PEDRO R. S. ANTUNES †, VINICIUS SANTOS ‡, AND PEDRO SERRANHO §

Abstract. The method of fundamental solutions (MFS) has been widely used to numerically solve boundary value problems involving linear partial differential equations. This method is easy to implement computationally and can be very effective for smooth domains and boundary conditions. The main drawback of the MFS is the ill-conditioning of the associated matrices, which may affect the method's accuracy. We present three methods to reduce the ill-conditioning of the classical MFS for the Laplace equation defined in bounded star-shaped domains in 3D. The idea is to expand the MFS basis functions in terms of spherical harmonics, in order to use the reduced QR factorization and singular value decomposition to deal with the ill-conditioning, leading to a better function basis that spans the same approximation space as the classical MFS. The numerical results illustrate that these approaches significantly decrease the ill-conditioning allowing higher accuracy when compared to the classical MFS.

Key words. method of fundamental solutions, ill-conditioning, Laplace equation

MSC codes. 65N20, 65N80 , 35J05

1. Introduction. The method of fundamental solutions (MFS) has been frequently used for the solution of boundary value problems governed by certain linear partial differential equations (PDEs). This method is well known for being truly meshfree and hence easier to implement [16]. It was first proposed by Kupradze and Aleksidze in the 1960's [22] and has been applied to several problems in acoustics [3, 2, 23], elasticity [9, 20], fluid dynamics [27, 19], or electromagnetism [15].

In two dimensions, the MFS may present spectral convergence under some regularity assumptions [21] and it is effective for solving PDEs. However, in the general case, there are still two issues hindering this method, namely its ill-conditioning and the choice of the source points. The best way to choose the source points has been widely studied [1, 6, 14], but to our knowledge there is no technique that significantly reduces the ill-conditioning of the matrices involved in the MFS for 3D domains.

Recently, a method capable of reducing the MFS ill-conditioning for the Laplace equation in planar domains was proposed in [5]. The idea is to consider expansions of MFS basis functions in terms of harmonic polynomial terms, then use singular value decomposition (SVD) and Arnoldi orthogonalization to produce a well-conditioned basis without changing the approximation space of the original MFS basis functions.

In this paper, we will present and analyze three methods to reduce the ill-

*Submitted to the editors.

Funding: The research of Pedro R. S. Antunes and Vinicius Santos was partially supported by FCT, Portugal, through the scientific project UIDB/00208/2020 (DOI: 10.54499/UIDB/00208/2020). The research of Pedro Serranho was partially funded by FCT, Portugal, through the scientific projects UIDB/04950/2020 (DOI: 10.54499/UIDB/04950/2020), UIDP/04950/2020 (DOI: 10.54499/UIDP/04950/2020), UIDB/04621/2020 (DOI: 10.54499/UIDB/04621/2020) and UIDP/04621/2020 (DOI: 10.54499/UIDP/04621/2020).

†Group of Mathematical Physics and Department of Mathematics, Instituto Superior Técnico, Av. Rovisco Pais 1, 1049-001 Lisboa, Portugal (prsantunes@tecnico.ulisboa.pt).

‡Group of Mathematical Physics, Av. Rovisco Pais 1, 1049-001 Lisboa, Portugal and Department of Science and Technology, Universidade Aberta, Rua da Escola Politécnica 141-147, Lisboa, Portugal.

§ Department of Science and Technology, Universidade Aberta, Rua da Escola Politécnica 141-147, Lisboa, Portugal and CIBIT, University of Coimbra, 3000-548 Coimbra, Portugal and CEMAT, University of Lisbon, Av. Rovisco Pais 1, 1049-001 Lisboa, Portugal (pedro.serranho@uab.pt).

conditioning of the MFS for bounded star-shaped domains in 3D which we will call the QR-MFS, SVD-MFS, and Hybrid-MFS. The first was inspired by a technique presented by Betcke and Trefethen in the context of the method of particular solutions for solving the Laplace eigenvalue problem [11], while the second and the third algorithms were adapted from [5].

The main idea of the QR-MFS is to work with an orthonormal basis constructed by a reduced QR factorization which span the same space of the original MFS basis functions. The SVD–MFS and Hybrid–MFS algorithms are complementary, the SVD–MFS may reduce considerably the ill-conditioning for smooth domains close to a ball. The Hybrid-MFS can remove the ill-conditioning in general domains. The idea in both algorithms is to consider an expansion of the MFS basis functions in terms of spherical harmonics. Details on the rationale and application of the methods will be given in section 3 and section 4.

The paper is organized as follows. In section 2 we describe the background of the classical MFS for the Laplace equation with Dirichlet boundary conditions. In section 3 we present the QR-MFS method. In section 4 we present the Laplace spherical harmonic expansion applied to the fundamental solution in 3D and the SVD–MFS and Hybrid–MFS. The numerical results are presented in section 5 and in section 6 we draw some conclusions and ideas for future work.

2. The Direct-MFS. We will consider the following boundary value problem for the Laplace equation with Dirichlet boundary conditions

$$\left\{ \begin{array}{rcll} \Delta u & = & 0 & \text{in} \quad \Omega \\ u & = & g & \text{on} \quad \partial\Omega \end{array} \right. \tag{2.1}$$

where Δ is the Laplace operator, $\Omega \subset \mathbb{R}^3$ is a bounded smooth domain and g is a given function defined on $\partial\Omega$.

We will refer to the classical MFS approach in [4, 5] as the Direct–MFS. We will briefly describe this method in the following lines. For more details we refer the readers to [16].

The Direct–MFS ansatz for the approximation u_{n_S} of the solution u of (2.1) is given by the following linear combination of fundamental solutions centered at n_S source points y_n.

$$u_{n_S}(x) = \sum_{n=1}^{n_S} \boldsymbol{c_n^D} \Phi(x, y_n), \quad x \in \bar{\Omega}, \quad y_n \in \partial\hat{\Omega} \tag{2.2}$$

where $\boldsymbol{c_n^D} \in \mathbb{R}$ are the coefficients to be determined, $\partial\hat{\Omega}$ is the boundary surface of the domain $\hat{\Omega}$ chosen such that $\bar{\Omega} \subset \hat{\Omega}$ and Φ is the fundamental solution of the Laplace equation given by

$$\Phi(x, y) = \tfrac{1}{4\pi\|x-y\|}, \quad x \neq y$$

where $\|x - y\|$ is the Euclidean distance between the points x and y.

Due to the properties of the fundamental solution, straightforward calculations show that the MFS approximation (2.2) satisfies the Laplace equation in Ω, so one needs to find the weights $\boldsymbol{c_n^D}, n = 1, 2, \ldots, n_S$, such that the boundary condition is satisfied. Therefore, we consider n_C collocation points $x_m \in \partial\Omega$, $m = 1, 2, \ldots, n_C$, and n_S source points $y_n \in \partial\hat{\Omega}$, $n = 1, 2, \ldots, n_S$, such that $n_C \geq n_S$ and impose the boundary condition by collocation, giving rise to the ill-conditioned linear system

$$A^{(C)}\boldsymbol{c^D} = \boldsymbol{b}, \tag{2.3}$$

where $A^{(C)}_{m,n} = \Phi(x_m, y_n)$ and $b_m = g(x_m)$ for $m = 1, 2, \ldots, n_C$, $n = 1, 2, \ldots, n_S$.

Having determined the solution $\boldsymbol{c^D}$ of (2.3), one can approximate the solution u by (2.2) at n_E evaluation points $z_p \in \bar{\Omega}$, $p = 1, 2, \ldots, n_E$, by the matrix product

$$\boldsymbol{v} = A^{(E)}\boldsymbol{c^D}, \tag{2.4}$$

where $A^{(E)}_{p,n} = \Phi(z_p, y_n)$ is the evaluation matrix for the MFS for $p = 1, 2, \ldots, n_E$, $n = 1, 2, \ldots, n_S$.

In the next section we describe a new approach for solving (2.2) inspired by [11] in the context of the method of particular solutions. An orthonormal basis is constructed by QR factorization considering collocation and evaluation points together.

3. QR-MFS. A way to solve the linear system (2.3) is to use the reduced QR factorization of the matrix $A^{(C)}$

$$A^{(C)} = QR$$

where $Q \in \mathbb{C}^{n_C \times n_S}$ is an orthonormal (by columns) matrix and $R \in \mathbb{C}^{n_S \times n_S}$ is a non-singular and upper-triangular matrix. Now we can rewrite (2.3) as

$$QR\boldsymbol{c^D} = \boldsymbol{b}. \tag{3.1}$$

We will now show that the matrix R is ill-conditioned. Having that in mind, we start by proving the following lemma

LEMMA 3.1. *Let $Q \in \mathbb{C}^{m\times n}$ be an orthonormal (by columns) matrix and $A \in \mathbb{C}^{p\times n}$ any matrix. Then $\|AQ^*\|_2 = \|A\|_2$.*

Proof. By Lemmas 7.3 and 7.2

$$\|AQ^*\|_2 = \|(AQ^*)^*\|_2 = \|QA^*\|_2 = \|A^*\|_2 = \|A\|_2. \qquad \square$$

For a matrix $A \in \mathbb{C}^{m\times n}$ of full rank, with $m \geq n$, we define the 2-norm condition number as in [26] by

$$k(A) = \|A\|_2\|A^+\|_2 \tag{3.2}$$

where A^+ denotes the pseudo-inverse of the matrix A which is the unique matrix that satisfies the following four conditions as indicated in [25]

$$A^+AA^+ = A^+, \tag{3.3a}$$

$$AA^+A = A, \tag{3.3b}$$

$$(AA^+)^* = AA^+, \tag{3.3c}$$

$$(A^+A)^* = A^+A. \tag{3.3d}$$

THEOREM 3.2. *Let $A = QR$ be the reduced QR factorization of a matrix $A \in \mathbb{C}^{m\times n}$, $m \geq n$, then $k(A) = k(R)$.*

Proof. We will assume that $(QR)^+ = R^+Q^*$ and under this assumption we will show that (3.3a)–(3.3d) hold, showing that R^+Q^* is the unique pseudo-inverse of QR. First we verify (3.3a)

$$(QR)^+QR(QR)^+ = R^+\underbrace{Q^*Q}_{I}RR^+Q^* = \underbrace{R^+RR^+}_{R^+}Q^* = R^+Q^* = (QR)^+.$$

Similarly, we have (3.3b)

$$QR(QR)^+QR = QRR^+\underbrace{Q^*Q}_{I}R = Q\underbrace{RR^+R}_{R} = QR.$$

Finally we have (3.3c)

$$(QR(QR)^+)^* = (QRR^+Q^*)^* = Q\underbrace{(RR^+)^*}_{RR^+}Q^* = QRR^+Q^* = QR(QR)^+$$

and (3.3d)

$$((QR)^+QR)^* = (R^+\underbrace{Q^*Q}_{I}R)^* = \underbrace{(R^+R)^*}_{R^+R} = R^+R = R^+\underbrace{Q^*Q}_{I}R = (QR)^+QR.$$

Therefore, using (3.2) and Lemmas 3.1 and 7.2 we get

$$k(A) = \|A\|_2\|A^+\|_2 = \|QR\|_2\|(QR)^+\|_2 = \|R\|_2\|R^+Q^*\|_2 = \|R\|_2\|R^+\|_2 = k(R).$$

∎

Since it is well-known that the MFS matrix A is ill-conditioned [13, 18, 17], the last result shows that R is also ill-conditioned. To avoid the ill-conditioning present in R, we define $\boldsymbol{c^{QR}} := R\boldsymbol{c^D}$, and then rewrite equation (3.1) as

$$Q\boldsymbol{c^{QR}} = \boldsymbol{b}$$

with the new coefficient vector $\boldsymbol{c^{QR}}$. We note that we will also need to evaluate the ansatz (2.2) at other evaluation points, so the reduced QR factorization should consider these evaluation points. We propose a method that will allow us to apply the new vector coefficient to solve problem (2.1) in a way to get around the ill-conditioning of R. We define

$$A = \begin{bmatrix} A^{(C)} \\ A^{(E)} \end{bmatrix}$$

and then we factorize A by reduced QR factorization ($A = QR$) where

$$Q = \begin{bmatrix} Q^{(C)} \\ Q^{(E)} \end{bmatrix}$$

and $Q^{(C)}$ and $Q^{(E)}$ have the same dimensions as $A^{(C)}$ and $A^{(E)}$, respectively, such that

$$A^{(C)} = Q^{(C)}R, \tag{3.4a}$$

$$A^{(E)} = Q^{(E)}R. \tag{3.4b}$$

By the definition of $\boldsymbol{c^{QR}}$ one now solves

$$Q^{(C)}\boldsymbol{c}^{\boldsymbol{QR}} = \boldsymbol{b} \tag{3.5}$$

instead of (2.3) and then calculates the approximation at the evaluation points as

$$\boldsymbol{v} = Q^{(E)}\boldsymbol{c}^{\boldsymbol{QR}}$$

instead of (2.4), avoiding the ill-conditioning of R.

Remark 3.3. The computational cost of the QR–MFS method is expected to be higher than the Direct–MFS, due to the additional QR decomposition. However, as illustrated in Tables 1 to 4 in section 5, this decomposition gives rise to less computational cost in solving the linear system (3.5), leading to similar CPU times to the Direct–MFS. In some cases (see Table 4) QR–MFS is even faster than the Direct-MFS.

Next, we will generalize the SVD-MFS introduced in [5] for star-shaped domains in 3D. In fact, we will propose two different methods for this problem depending on the shape of the domain, namely the SVD–MFS and the Hybrid–MFS.

4. Laplace spherical harmonic expansion. In this section, we will describe the SVD–MFS and Hybrid–MFS applied to 3D domains. The main idea in the SVD–MFS method is to expand the MFS basis functions in terms of spherical harmonics, and then use the SVD to change the basis. The idea in the Hybrid–MFS is to combine ideas from the SVD-MFS and QR-MFS. Actually, it is similar to the SVD-MFS, but uses a reduced QR factorization and a SVD on the ill-conditioned part of that factorization. In this section we will need the following assumption.

ASSUMPTION 4.1. *We will assume there exists a ball* B^{Ω} *such that* $\Omega \subset B^{\Omega} \subset \hat{\Omega}$.

We consider the transformation from cartesian coordinates (x_1, x_2, x_3) to spherical coordinates (ρ, θ, ϕ) given by

$$(x_1, x_2, x_3) = (\rho\cos(\phi)\sin(\theta), \rho\sin(\phi)\sin(\theta), \rho\cos(\theta))$$

where $\rho \in [0, +\infty[$, $\theta \in [0, \pi]$ and $\phi \in [-\pi, \pi[$.

Let $x = (r, \omega, \varphi)$ be a collocation point and $y = (R, \varepsilon, \eta)$ a source point in spherical coordinates. We can use the Laplace spherical harmonic expansion from [8] to get

$$\begin{aligned}\frac{1}{4\pi\|x-y\|} &= \sum_{k=0}^{\infty}\frac{1}{2k+1}\frac{r^k}{R^{k+1}}\sum_{m=-k}^{k}\overline{Y_k^m(\omega,\varphi)}Y_k^m(\varepsilon,\eta) \\ &= \sum_{k=0}^{\infty}\sum_{m=-k}^{k}\frac{r_\Omega^k}{2k+1}\frac{Y_k^m(\varepsilon,\eta)}{R^{k+1}}\frac{r^k\overline{Y_k^m(\omega,\varphi)}}{r_\Omega^k}\end{aligned} \tag{4.1}$$

where for convenience we multiplied and divided each term in the sum by $r_\Omega^k := \max_{x\in\partial\Omega}\|x\|$, and the spherical harmonics [24, 10] are given by

$$Y_k^m(\theta,\phi) = (-1)^m\sqrt{\frac{2k+1}{4\pi}\frac{(k-m)!}{(k+m)!}}p_k^m(\cos\theta)e^{im\phi}$$

where p_k^m are the associated Legendre functions

$$p_k^m(t) = (1-t^2)^{m/2}\frac{d^m}{dt^m}P_k(t), \quad m = 0, 1, \ldots, k,$$

that are extended to $-k \leq m \leq k$ as follows

$$p_k^m(t) = \frac{(k-m)!}{(k+m)!} p_k^{|m|}(t),$$

and $P_k(t)$ are the Legendre polynomial of degree k, given by

$$P_k(t) = \frac{1}{2^k k!} \frac{d^k}{dx^k}(t^2-1)^k.$$

Therefore, we can expand the MFS basis functions $\Phi(x, y_j)$ associated to a sample of n source points as

$$\begin{bmatrix} \Phi(x,y_1) \\ \Phi(x,y_2) \\ \vdots \\ \Phi(x,y_n) \end{bmatrix} =$$

$$\begin{bmatrix} \frac{1}{R_1^1} Y_0^0(\varepsilon_1,\eta_1) \frac{r_\Omega^0}{1} & \dots & \frac{1}{R_1^{k+1}} Y_k^m(\varepsilon_1,\eta_1) \frac{r_\Omega^k}{2k+1} & \dots & \\ \frac{1}{R_2^1} Y_0^0(\varepsilon_2,\eta_2) \frac{r_\Omega^0}{1} & \dots & \frac{1}{R_2^{k+1}} Y_k^m(\varepsilon_2,\eta_2) \frac{r_\Omega^k}{2k+1} & \dots & \\ \vdots & \vdots & \vdots & \vdots & \ddots \\ \frac{1}{R_n^1} Y_0^0(\varepsilon_n,\eta_n) \frac{r_\Omega^0}{1} & \dots & \frac{1}{R_n^{k+1}} Y_k^m(\varepsilon_n,\eta_n) \frac{r_\Omega^k}{2k+1} & \dots & \end{bmatrix} \begin{bmatrix} \frac{r^0(\theta,\phi)}{r_\Omega^0} \overline{Y_0^0(\omega,\varphi)} \\ \vdots \\ \frac{r^k(\theta,\phi)}{r_\Omega^k} \overline{Y_k^m(\omega,\varphi)} \\ \vdots \end{bmatrix}$$

where the n^{th} source point is defined by $y_n = (R_n, \varepsilon_n, \eta_n)$. After truncating this expansion, considering the sum in (4.1) just up to $k = \mathcal{K}$ we get

$$\frac{1}{4\pi\|x-y\|} \approx \sum_{k=0}^{\mathcal{K}} \sum_{m=-k}^{k} \frac{r_\Omega^k}{2k+1} \frac{Y_k^m(\varepsilon,\eta)}{R^{k+1}} \frac{r^k \overline{Y_k^m(\omega,\varphi)}}{r_\Omega^k}. \tag{4.2}$$

Considering $\boldsymbol{\alpha}$ as the following vector

$$\boldsymbol{\alpha} = \begin{bmatrix} \Phi(x,y_1) & \Phi(x,y_2) & \dots & \Phi(x,y_n) \end{bmatrix}$$

we can write the factorization $\boldsymbol{\alpha}^{\mathrm{T}} \approx MF$ where $\boldsymbol{\alpha}^{\mathrm{T}}$ is transpose of the vector $\boldsymbol{\alpha}$,

$$M = \begin{bmatrix} \frac{1}{R_1^1} Y_0^0(\varepsilon_1,\eta_1) \frac{r_\Omega^0}{1} & \dots & \frac{1}{R_1^{\mathcal{K}+1}} Y_{\mathcal{K}}^{-\mathcal{K}}(\varepsilon_1,\eta_1) \frac{r_\Omega^{\mathcal{K}}}{2\mathcal{K}+1} & \dots & \frac{1}{R_1^{\mathcal{K}+1}} Y_{\mathcal{K}}^{\mathcal{K}}(\varepsilon_1,\eta_1) \frac{r_\Omega^{\mathcal{K}}}{2\mathcal{K}+1} \\ \frac{1}{R_2^1} Y_0^0(\varepsilon_2,\eta_2) \frac{r_\Omega^0}{1} & \dots & \frac{1}{R_2^{\mathcal{K}+1}} Y_{\mathcal{K}}^{-\mathcal{K}}(\varepsilon_2,\eta_2) \frac{r_\Omega^{\mathcal{K}}}{2\mathcal{K}+1} & \dots & \frac{1}{R_2^{\mathcal{K}+1}} Y_{\mathcal{K}}^{\mathcal{K}}(\varepsilon_2,\eta_2) \frac{r_\Omega^{\mathcal{K}}}{2\mathcal{K}+1} \\ \vdots & \vdots & \vdots & \ddots & \vdots \\ \frac{1}{R_n^1} Y_0^0(\varepsilon_n,\eta_n) \frac{r_\Omega^0}{1} & \dots & \frac{1}{R_n^{\mathcal{K}+1}} Y_{\mathcal{K}}^{-\mathcal{K}}(\varepsilon_n,\eta_n) \frac{r_\Omega^{\mathcal{K}}}{2\mathcal{K}+1} & \dots & \frac{1}{R_n^{\mathcal{K}+1}} Y_{\mathcal{K}}^{\mathcal{K}}(\varepsilon_n,\eta_n) \frac{r_\Omega^{\mathcal{K}}}{2\mathcal{K}+1} \end{bmatrix}$$

and

$$F = \begin{bmatrix} \frac{r^0(\theta,\phi)}{r_\Omega^0} \overline{Y_0^0(\omega,\varphi)} \\ \vdots \\ \frac{r^{\mathcal{K}}(\theta,\phi)}{r_\Omega^{\mathcal{K}}} \overline{Y_{\mathcal{K}}^{-\mathcal{K}}(\omega,\varphi)} \\ \vdots \\ \frac{r^{\mathcal{K}}(\theta,\phi)}{r_\Omega^{\mathcal{K}}} \overline{Y_{\mathcal{K}}^{\mathcal{K}}(\omega,\varphi)} \end{bmatrix} \tag{4.3}$$

where F is a vector-valued function with $(\mathcal{K}+1)^2$ rows. Note that for each integer k starting at zero, we have $2k+1$ terms in the interior sum in (4.2) corresponding to the spherical harmonics of order k, that is, a total of $(\mathcal{K}+1)^2$ terms in (4.2).

Remark 4.2. In the following line, it is important to refer to the non singularity of M. Since it is known that the spherical harmonics are linearly independent, one can choose a set of source points that guarantees the matrix

$$\begin{bmatrix} Y_0^0(\varepsilon_1,\eta_1) & \dots & Y_k^m(\varepsilon_1,\eta_1) & \dots & \\ Y_0^0(\varepsilon_2,\eta_2) & \dots & Y_k^m(\varepsilon_2,\eta_2) & \dots & \\ \vdots & \vdots & \vdots & \vdots & \ddots \\ Y_0^0(\varepsilon_n,\eta_n) & \dots & Y_k^m(\varepsilon_n,\eta_n) & \dots & \end{bmatrix}$$

is non singular. Moreover, matrix M is obtained by multiplying each column k of this previous matrix by the constant $\frac{r_\Omega^k}{2k+1}$, therefore preserving the non singularity. However, to obtain the matrix M each entry (n,k) is multiplied by the factor $\frac{1}{R_n^{k+1}}$. Therefore, one can only assure the non singularity of M if the source points are on a circle, since in that case $R_1 = R_2 = \cdots = R_n$, and the same argument holds. Since one controls the position of the source points, this assumption can be assured.

To determine the value $\mathcal{K}$ we use the spherical harmonic addition theorem from [8] to ensure that the remainder is small enough.

We consider

$$P_k(\cos\Theta) = \frac{4\pi}{2k+1}\sum_{m=-k}^{k} \overline{Y_k^m(\omega,\varphi)}\, Y_k^m(\varepsilon,\eta)$$

where Θ is the angle between (r,ω,φ) and (R,ε,η). So, we can rewrite the equation (4.1) as

$$\frac{1}{4\pi\|x-y\|} = \frac{1}{R}\sum_{k=0}^{\infty}\left(\frac{r}{R}\right)^k \frac{P_k(\cos\Theta)}{4\pi},$$

and thus

$$\left|\frac{1}{\|x-y\|} - \frac{1}{R}\sum_{k=0}^{\mathcal{K}}\left(\frac{r}{R}\right)^k P_k(\cos\Theta)\right| \le \frac{1}{R}\sum_{k=\mathcal{K}+1}^{\infty}\left(\frac{r}{R}\right)^k |P_k(\cos\Theta)|.$$

Now, we can use the fact that $|P_k(\cos\Theta)| \le 1$ for any $\Theta \in [0,2\pi]$ as in [7] and write the following inequality

$$\left|\frac{1}{\|x-y\|} - \frac{1}{R}\sum_{k=0}^{\mathcal{K}}\left(\frac{r}{R}\right)^k P_k(\cos\Theta)\right| \le \frac{1}{R}\sum_{k=\mathcal{K}+1}^{\infty}\left(\frac{r}{R}\right)^k \le \epsilon \tag{4.4}$$

where ϵ is the desired machine precision. From the geometric series in (4.4), we get the lower bound

$$\mathcal{K} \ge \left\lceil \frac{\ln\left(\epsilon(R-r)\right)}{\ln\frac{r}{R}} - 1 \right\rceil$$

where we define

$$\mathcal{K}_0 = \left\lceil \frac{\ln\left(\epsilon(R-r)\right)}{\ln\frac{r}{R}} - 1 \right\rceil.$$

Given the same sample of n_C collocation points, n_E evaluation points and n_S source points used in the Direct-MFS, we can write

$$(A^{(C)})^{\mathrm{T}} = MF^{(C)} \tag{4.5}$$

$$(A^{(E)})^{\mathrm{T}} = MF^{(E)} \tag{4.6}$$

where $F^{(C)} \in \mathbb{C}^{(\mathcal{K}_0+1)^2 \times n_C}$ and $F^{(E)} \in \mathbb{C}^{(\mathcal{K}_0+1)^2 \times n_E}$ are matrices built from F in (4.3), respectively, with the collocation and evaluation points in spherical coordinates. Note that there is an abuse of notation in the sense that the equal sign in (4.5) and (4.6) corresponds to an equality up to machine precision accuracy, due to the truncation of the series.

4.1. SVD-MFS. For the time being, let us assume that $F^{(C)}$ is well-conditioned, keeping in mind that this is the case for a spherical domain, since for the ball we have that $\frac{r}{r_\Omega} = 1$, hence, the components of $F^{(C)}$ reduce to spherical harmonics that are orthogonal, which means that $F^{(C)}$ is well–conditioned. Therefore, we will focus on treating the ill-conditioning of M.

Here, we assume that $\mathcal{K}$ is chosen such that $(\mathcal{K}+1)^2 \geq n_S$, and therefore, define

$$\mathcal{K}_1 := \max\left(\mathcal{K}_0, \lceil \sqrt{n_S} - 1 \rceil\right).$$

The SVD-MFS technique for reducing the effect of the ill-conditioning of matrix M consists of the following steps. First, we calculate the singular value decomposition of matrix M

$$M = USV^*$$

where U and V are unitary and S is diagonal with non-negative entries. Then, multiplying by U^* from the left we obtain

$$U^*M = U^*USV^* = SV^*. \tag{4.7}$$

The matrix S has the same dimensions of M, that is M has n_S rows and $(\mathcal{K}_1+1)^2$ columns. Therefore,

$$S = \begin{bmatrix} S_1 \mid 0 \end{bmatrix}$$

where S_1 is a diagonal square matrix and 0 denotes a block zero matrix and thus

$$SV^* = \begin{bmatrix} S_1 \mid 0 \end{bmatrix} \begin{bmatrix} V_1^* \\ \overline{V_2^*} \end{bmatrix} = S_1V_1^* + 0V_2^* = S_1V_1^*$$

where V_1^* is the matrix composed of the first n rows of V^*. Now, keeping in mind remark 4.2, one can assume that S_1 is non singular, so multiplying equation (4.7) by matrix S_1^{-1} from the left, we get

$$S_1^{-1}SV^* = S_1^{-1}S_1V_1^* = V_1^*. \tag{4.8}$$

Thus, multiplying (4.5) by the matrix $S_1^{-1}U^*$ from the left, we obtain a new set of basis functions without modifying its functional space span. Therefore we get

$$S_1^{-1}U^*(A^{(C)})^T = S_1^{-1}U^*MF^{(C)}$$

which by equations (4.7) and (4.8) is the same as

$$S_1^{-1}U^*(A^{(C)})^T = V_1^*F^{(C)}$$

hence, taking the transpose, we have

$$A^{(C)}(U^*)^T(S_1^{-1})^T = (V_1^*F^{(C)})^T.$$

So, multiplying it by $(S_1)^TU^T$ from the right

$$A^{(C)} = (V_1^*F^{(C)})^T(S_1)^TU^T. \tag{4.9}$$

Plugging (4.9) into (2.3) we get

$$(V_1^*F^{(C)})^T\boldsymbol{c^{SVD}} = \boldsymbol{b} \tag{4.10}$$

where $\boldsymbol{c^{SVD}} := (S_1)^TU^T\boldsymbol{c^D}$. In a similar way, we get

$$A^{(E)} = (V_1^*F^{(E)})^T(S_1)^TU^T. \tag{4.11}$$

Plugging (4.11) into (2.4) we get the approximation at the evaluation points by

$$\boldsymbol{v} = (V_1^*F^{(E)})^T\boldsymbol{c^{SVD}}.$$

where $\boldsymbol{c^{SVD}}$ is the solution of (4.10).

Remark 4.3. This method has a higher computational cost than both the Direct–MFS and the QR–MFS, not only because it requires building larger matrices due to the addition theorem, but essentially also due to the computing of a SVD factorization.

In the next subsection, we will show how to remove the ill-conditioning of matrix $F^{(C)}$.

4.2. Hybrid-MFS. Let us now assume that, in contrast to the case treated in subsection 4.1, $F^{(C)}$ is ill-conditioned. In this case, the idea is to rewrite matrix $F^{(C)}$ with an orthonormal basis using reduced QR factorization and dealing with the ill-conditioning of $F^{(C)}$ through SVD. In this way, one needs to consider simultaneously the evaluation and collocation points. Given the same n_C collocation points and n_E evaluation points as in the Direct–MFS we define

$$P = \begin{bmatrix}(F^{(C)})^T\\(F^{(E)})^T\end{bmatrix},$$

therefore P has $n_C + n_E$ rows and $(\mathcal{K}_1+1)^2$ columns.

Using the reduced QR factorization of P, one can write

$$P = \begin{bmatrix}(Q^{(C)})^T\\(Q^{(E)})^T\end{bmatrix}R$$

where $Q^{(C)}$ and $Q^{(E)}$ have the same dimensions as $F^{(C)}$ and $F^{(E)}$, respectively.

Therefore, taking the transpose of P, we have

$$P^T = \begin{bmatrix}R^TQ^{(C)} & R^TQ^{(E)}\end{bmatrix}$$

where

$$F^{(C)} = R^TQ^{(C)} \tag{4.12}$$

$$F^{(E)} = R^TQ^{(E)}. \tag{4.13}$$

Plugging (4.12) into equation (4.5) we have

$$(A^{(C)})^T = MR^T Q^{(C)} = \tilde{M} Q^{(C)} \tag{4.14}$$

where $\tilde{M} := MR^T$, and from the SVD of $\tilde{M}$ we get the matrices $\tilde{S}_1^{-1}$ and $\tilde{U}^*$ as in subsection 4.1. Multiplying the equation (4.14) by $\tilde{S}_1^{-1}\tilde{U}^*$ from the left one gets

$$\tilde{S}_1^{-1}\tilde{U}^*(A^{(C)})^T = \tilde{S}_1^{-1}\tilde{U}^*\tilde{M}Q^{(C)} = \tilde{V}_1 Q^{(C)}$$

that leads to

$$A^{(C)} = (\tilde{V}_1^* Q^{(C)})^T (\tilde{S}_1)^T \tilde{U}^T \tag{4.15}$$

and plugging (4.15) into equation (2.3) we have

$$(\tilde{V}_1^* Q^{(C)})^T \boldsymbol{c^H} = \boldsymbol{b} \tag{4.16}$$

where $\boldsymbol{c^H} := (\tilde{S}_1)^T \tilde{U}^T \boldsymbol{c^D}$. Following the same steps, plugging (4.13) into (4.6), we have

$$A^{(E)} = (\tilde{V}_1^* Q^{(E)})^T (\tilde{S}_1)^T \tilde{U}^T, \tag{4.17}$$

hence plugging (4.17) into (2.4) we get the approximation at the evaluation points

$$\boldsymbol{v} = (\tilde{V}_1^* Q^C)^T \boldsymbol{c^H}$$

where $\boldsymbol{c^H}$ is the solution of (4.16).

Remark 4.4. The computational cost of this method is higher than all the previously presented approaches, since it involves building large matrices due to the addition theorem and requires computing two factorizations.

Since the Hybrid–MFS is more complex than previous the approaches, we summarize the procedure in Algorithm 4.1.

Algorithm 4.1 Hybrid–MFS

1. Choose $n_S \in \mathbb{N}$, the number of basis functions.
2. Place $n_C > n_S$ collocation points on $\partial\Omega$.
3. Choose n_S source points such that Assumption 4.1 holds.
4. Calculate $\mathcal{K}_1 \in \mathbb{N}$.
5. Build the matrices $B, D, F^{(C)}$ and $F^{(E)}$.
6. Define P.
7. Calculate the reduced QR factorization of P.
8. Define $\tilde{M}$.
9. Compute the singular value decomposition of $\tilde{M}$ to obtain $\tilde{V}_1^*$.
10. Compute the linear system of the Hybrid–MFS.
11. Solve the linear system to calculate the Hybrid–MFS coefficients.
12. Evaluate the solution at the evaluation points through $F^{(E)}$.

5. Numerical results. We present numerical results for the unit ball and three other domains (see Figure 1) to compare the Direct–MFS and the proposed methods for non-harmonic boundary conditions on three-dimensional domains, since it is known that this case is more challenging in terms of convergence than the case of harmonic solutions. In all the examples the Dirichlet boundary conditions are given by $g(x, y, z) = x^2y^2z^2$, and the source points were fixed on a sphere of radius $R = 3$. In all examples we took $n_C \approx 3n_S$, except for the Example 5.3 where due to the complexity of the domain more collocation points are needed. In this case we chose $n_C \approx 7n_S$.

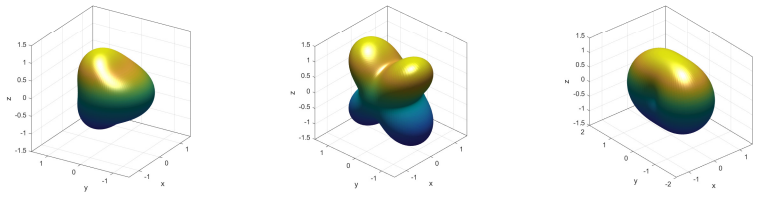

(a) (b) (c)

Fig. 1: Plot of domains considered in Example 5.2(a), Example 5.4(b) and Example 5.3(c).

In order to satisfy Assumption 4.1, the source points for our approaches are considered to be far from the domain. However, this does not favour the Direct–MFS. Indeed, some works in the literature [12, 14] suggest that the Direct–MFS performance is better when the artificial boundary is similar and close to the real boundary. The Effective Condition Number Method (ECNM), presented in [12], provides an efficient way to determine the location of the source points. Therein, approach 1 involves using the ECNM with source points placed on a spherical surface of radius R, while approach 2 involves using source points on a dilated boundary with a magnification factor τ. Therefore for a fair comparison with the Direct–MFS, we compare the performance of our approaches also with approaches 1 and 2 in [12]. As expected, these methods require solving optimization problems to determine the value of R or τ which may justify the high computational cost.

In each of the examples below, we provide a table that illustrates the performance of Direct-MFS, QR–MFS, SVD-MFS, and Hybrid-MFS, as well as approach 1 and approach 2 in [12]. The goal is to assess the impact of maintaining $R = 3$ in the methods described here.

By the maximum principle, since u and u_{n_S} are both harmonic functions we have

$$\|u - u_{n_S}\|_{L^\infty(\Omega)} \leq \|u - u_{n_S}\|_{L^\infty(\partial\Omega)} = \|g - u_{n_S}\|_{L^\infty(\partial\Omega)}.$$

To estimate the error we consider the discrete ℓ^∞-norm over $\partial\Omega$ at around 10000 boundary points.

The numerical experiments in this section were carried out using Matlab software on a notebook PC with 11th Gen Intel(R) Core(TM) i7-1165G7 @ 2.80GHz, 20GB RAM, on Windows 11.

For all examples we consider smooth star-shaped domains with boundary given

by

$$\partial\Omega = \{(x,y,z) = r(\theta,\phi)(\cos(\phi)\sin(\theta), \sin(\phi)\sin(\theta), \cos(\theta)), \\ 0 \leq \theta \leq \pi, -\pi \leq \phi < \pi\} \tag{5.1}$$

where $r(\theta,\phi)$ represents the radial function.

Example 5.1. We consider Ω as the unit sphere.

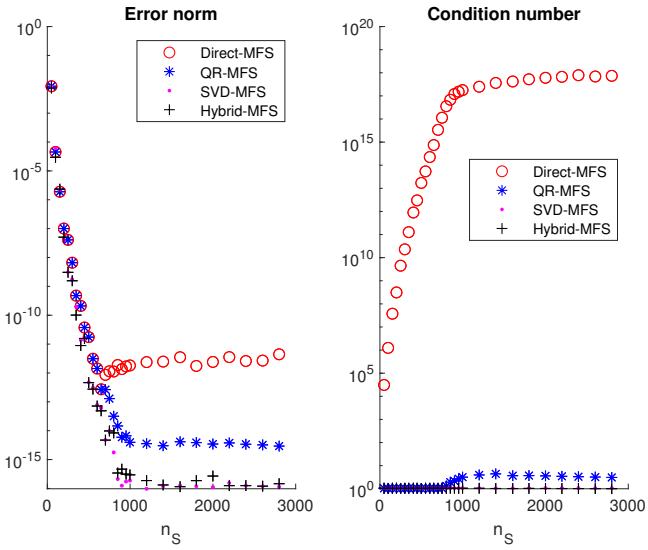

Fig. 2: Plot of the ℓ^∞ norm of the error on the boundary of the numerical approximations given by the Direct–MFS, QR–MFS, SVD–MFS, and Hybrid–MFS, as a function of n_S (left plot) and plot of the condition number of the matrix of the linear systems (right plot) of Example 5.1.

We observe in Figure 2 that the L^∞ norm of the error converges fast to zero with the increase of n_S. In all approaches the numerical results are similar for $n_S < 900$. For larger n_S the Direct–MFS does not improve, due to the ill-conditioning, while our approaches reach machine precision.

Note that in the right plot of the Figure 2 the condition numbers of the SVD–MFS and Hybrid–MFS methods do not increase with n_S, being approximately equal to 1.

In Table 1, we present the numerical results of Example 5.1 where we took $n_S = 2000$ and $n_C = 6007$. The search interval for both the optimal value of the radius R of the sphere in approach 1, and the magnification factor τ in approach 2 was $[1.01, 3.8]$. The minimum value needed to truncate the right side of the equation (4.1) was $\mathcal{K}_0 = 31$.

Example 5.2. We change the geometry defined in Example 5.1 to a more complex one. We consider the reduced bumpy sphere (see Figure 1a) as in example 8 of [16], where $r(\theta,\phi) = 1 + \frac{1}{6}\sin(\theta)\cos(3\phi)$ in equation (5.1).

In Figure 3, we note that as in example 1 for $n_S < 1000$ the numerical results obtained are similar for all approaches. However, for $n_S > 1000$ due to the

Table 1: Condition number, error norm and CPU times for the considered approaches for the unit sphere (Example 5.1) with $n_S = 2000$ and $n_C = 6007$.

	Condition number		l^∞-norm over $\partial\Omega$	CPU time (s)
Direct–MFS	6.0682e+17	$R = 3$	2.4130e-12	9.4
Approach 1 - [12]	3.9716e+17	$R = 2.4713$	9.8450e-13	87.9
Approach 2 - [12]	2.7879e+16	$\tau = 1.9611$	2.0859e-13	84.7
QR–MFS	3.6198	$R = 3$	3.4556e-15	9.7
SVD–MFS	1.0713	$R = 3$	9.7757e-17	31.6
Hybrid–MFS	1.0283	$R = 3$	1.7687e-16	42.3

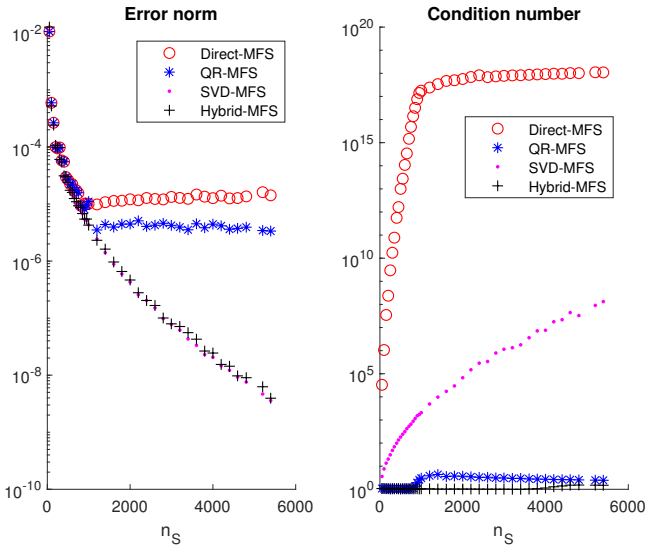

Fig. 3: Plot of the L^∞ norm of the error on the boundary of the numerical approximations given by the Direct–MFS, QR–MFS, SVD–MFS, and Hybrid–MFS, as a function of n_S (left plot) and plot of the condition number of the matrix of the linear systems (right plot) of Example 5.2

.

ill-conditioning the convergence of the Direct–MFS breaks down while the L^∞ norm of the error of SVD–MFS and Hybrid–MFS continues decreasing. Surprisingly QR–MFS also does not improve for larger n_S despite the low condition number.

In Table 2, we present the numerical results of Example 5.2 where we took $n_S = 2996$ and $n_C = 8998$. The search interval for the optimal value of the radius R of the sphere in approach 1 was $[1.5, 3.8]$, and for the magnification factor τ in approach 2 was $[1.01, 3.8]$. The minimum value needed to truncate the right side of the equation (4.1) was $\mathcal{K}_0 = 36$.

Example 5.3. We consider a cushion shaped domain (see Figure 1b) that is star-like with a radial function given by

$$r(\theta, \phi) = \sqrt{0.8 + 0.5(\cos(2\theta) - 1)(\cos(4\phi) - 1)}.$$

Table 2: Condition number, error norm and CPU times for the considered approaches for the reduced bumpy sphere (Example 5.2) with $n_S = 2996$ and $n_C = 8998$

	Condition number		l^∞-norm over $\partial\Omega$	CPU time (s)
Direct–MFS	7.7771e+17	$R = 3$	1.3322e-05	23.0
Approach 1 - [12]	6.0329e+16	$R = 1.6622$	1.1469e-07	383.2
Approach 2 - [12]	2.0813e+16	$\tau = 1.6946$	1.0259e-07	427.0
QR–MFS	3.0847	$R = 3$	4.2299e-06	25.7
SVD–MFS	1.0843e+06	$R = 3$	7.8038e-08	152.3
Hybrid–MFS	1.0097	$R = 3$	7.9151e-08	154.8

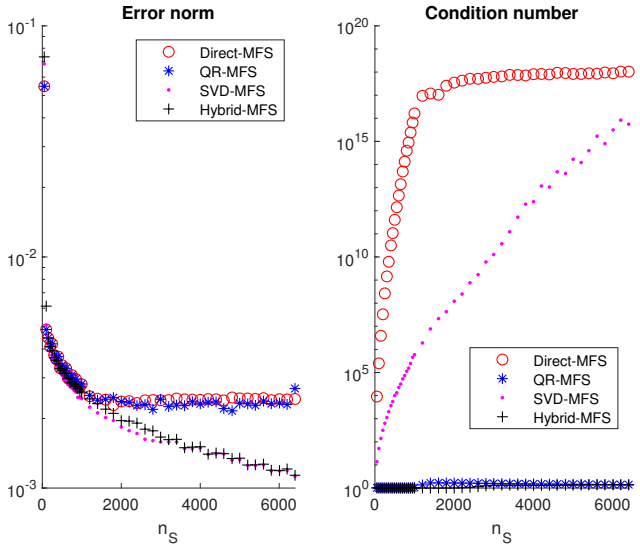

Fig. 4: Plot of the L^∞ norm of the error on the boundary of the numerical approximations given by the Direct–MFS, QR–MFS, SVD–MFS, and Hybrid–MFS, as a function of n_S (left plot) and plot of the condition number of the matrix of the linear systems (right plot) of Example 5.3.

Figure 4 illustrates that the behaviour of the numerical results is similar to Example 5.2. The Direct–MFS and QR–MFS convergence breaks down for $n_S > 1000$. We can see that the condition number of the SVD–MFS grows slowly and has still no effect on convergence.

The Hybrid–MFS continues to improve the results with increasing of the n_S, with the condition number remaining approximately equal to 1.3 for $n_S = 6400$.

In Table 3, we present the numerical results of Example 5.3 where we took $n_S = 2000$ and $n_C = 14003$. The search interval for the optimal value of the radius R of the sphere in approach 1 was $[1.8, 3.8]$, and for the magnification factor τ in approach 2 was $[1.01, 3.8]$. The minimum value needed to truncate the right side of the equation (4.1) was $\mathcal{K}_0 = 59$.

Example 5.4. In the last example, the boundary geometry is a pinched ball (see Figure 1c) with a radial function in equation (5.1) given by

Table 3: Condition number, error norm and CPU times for the considered approaches for the cushion (Example 5.3) with $n_S = 2000$ and $n_C = 14003$

	Condition number		l^∞-norm over $\partial\Omega$	CPU time (s)
Direct–MFS	3.4883e+17	$R = 3$	2.4e-3	21.8
Approach 1 - [12]	8.1543e+16	$R = 2.1480$	2.2e-3	337.4
Approach 2 - [12]	1.1405e+17	$\tau = 1.9283$	2.2e-3	312.1
QR–MFS	1.6522	$R = 3$	2.4e-3	20.6
SVD–MFS	1.5741e+08	$R = 3$	1.8e-3	90.2
Hybrid–MFS	1.0040	$R = 3$	2.0e-3	148.6

$$r(\theta, \phi) = \sqrt{1.44 + 0.5(\cos 2\theta)(\cos(2\phi) - 1)}. \tag{387}$$

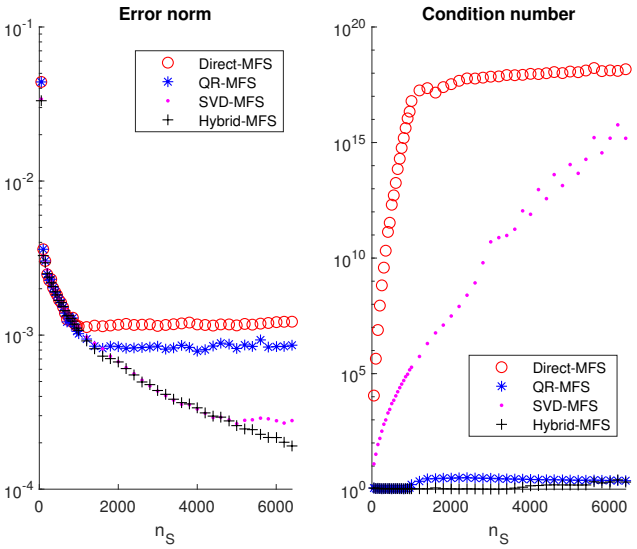

Fig. 5: Plot of the L^∞ norm of the error on the boundary of the numerical approximations given by the Direct–MFS, QR–MFS, SVD–MFS, and Hybrid–MFS, as a function of n_S (left plot) and plot of the condition number of the matrix of the linear systems (right plot) of Example 5.4.

388

389 Figure 5 illustrates that the condition number of the Direct–MFS grows rapidly
390 such that for $n_S > 1000$ the solution error becomes constant and does not improve
391 anymore. Though the conditioning of the QR-MFS remains good, the error of the
392 solution also becomes stable, though better than the Direct–MFS.
393 The SVD–MFS reduces ill-conditioning when we compare it with the Direct–
394 MFS and at the same time improves the solution until $n_S \approx 5000$. For larger n_S
395 the SVD-MFS convergence breaks down due to ill-conditioning while the Hybrid–
396 MFS convergence continues, since the condition number of the Hybrid–MFS remains
397 approximately equal to 2.

In Table 4, we present the numerical results of Example 5.4 where we took $n_S = 6007$ and $n_C = 18004$. The search interval for the optimal value of the radius R of the sphere in approach 1 was $[1.7, 3.8]$, and for the magnification factor τ in approach 2 was $[1.01, 3.8]$. The minimum value needed to truncate the right side of the equation (4.1) was $\mathcal{K}_0 = 53$.

Table 4: Condition number, error norm and CPU times for the considered approaches for the pinched ball (Example 5.4) with $n_S = 6007$ and $n_C = 18004$

	Condition number		l^∞-norm over $\partial\Omega$	CPU time (s)
Direct–MFS	1.3210e+18	$R = 3$	1.2e-3	192.8
Approach 1 - [12]	1.9389e+18	$R = 2.3875$	8.4386e-04	2813.4
Approach 2 - [12]	1.4956e+15	$\tau = 1.3939$	1.8104e-05	2787.7
QR–MFS	2.3792	$R = 3$	8.4241e-04	186.2
SVD–MFS	1.4956e+15	$R = 3$	2.7450e-04	933.8
Hybrid–MFS	2.0256	$R = 3$	2.1554e-04	1194.6

6. Conclusions. We proposed three methods for reducing the ill-conditioning of the Direct–MFS for general star-shaped domains in 3D provided that the source points satisfy Assumption 4.1. Our methods alter the original MFS basis functions to a basis using SVD or reduced QR factorization spanning the same space and leading to a better conditioned linear system. Numerical results suggest that the performance of the methods can be sorted. In fact, QR-MFS, though clearly outperforming the Direct-MFS, seems to have a poorer performance than SVD-MFS and Hybrid-MFS. Also, in some cases (see Example 5.4), the Hybrid-MFS seems to be the best choice in terms of accuracy, since the condition number stays bounded. However, it has a higher computational cost, since it requires the use of two factorizations instead of just one, as in the QR-MFS and SVD-MFS. It is also worth mentioning that the QR-MFS presents similar computation times to the Direct–MFS, despite the additional factorization.

In the examples considered our methods perform better than approaches 1 and 2 of [12], except in the example 5.3 for which approaches 1 and 2 are slightly better. However, those approaches present higher computation time than the proposed methods due to the optimization process for finding the optimal location of the source points.

With our approaches one can improve the accuracy by considering a larger number of both collocation and source points that would be impossible for the Direct–MFS due to ill-conditioning. Moreover, one can consider a larger family of artificial boundaries since the ill-conditioning is highly reduced by the proposed approaches. For instance, artificial boundaries far from the domain that for Direct–MFS lead to severely ill-conditioned linear systems can now be applied with our proposed methods. On the down side, the SVD–MFS and Hybrid–MFS hold only under Assumption 4.1.

In terms of future work, it is expected that a similar approach can be considered for other elliptic PDEs. Moreover, these approaches open new possibilities and open problems in terms of the choice of source points. On one side, it seems that these approaches clearly overcome the performance of the wisest choice of source points for the Direct–MFS. On the other side, the optimal choice of source points for reducing the ill-conditioning of the direct MFS might not generate the optimal basis functions by our approach. This is an open problem that might also be considered in the future.

7. Appendix. In this appendix we list some trivial linear algebra results supporting the results in section 3.

We define the 2-norm of an $m \times n$ matrix A by

$$\|A\|_2 = \sup_{\substack{\boldsymbol{x} \in \mathbb{C}^n \\ \boldsymbol{x} \neq 0}} \frac{\|A\boldsymbol{x}\|}{\|\boldsymbol{x}\|}, \tag{7.1}$$

where $\|.\|$ is the Euclidean norm in $\mathbb{C}^n$.

LEMMA 7.1. *Let $Q \in \mathbb{C}^{m\times n}$ be an orthonormal (by columns) matrix and $\boldsymbol{x} \in \mathbb{C}^{n\times 1}$ be a vector. Then $\|Q\boldsymbol{x}\| = \|\boldsymbol{x}\|$.*

Proof. We have that

$$\|Q\boldsymbol{x}\| = \sqrt{(Q\boldsymbol{x})^* Q\boldsymbol{x}} = \sqrt{\boldsymbol{x}^* Q^* Q\boldsymbol{x}} = \sqrt{\boldsymbol{x}^* I\boldsymbol{x}} = \sqrt{\boldsymbol{x}^*\boldsymbol{x}} = \|\boldsymbol{x}\|. \qquad \square$$

LEMMA 7.2. *Let $Q \in \mathbb{C}^{m\times n}$ be an orthonormal (by columns) matrix and $A \in \mathbb{C}^{n\times p}$ any matrix. Then $\|QA\|_2 = \|A\|_2$.*

Proof. By (7.1) and Lemma 7.1

$$\|QA\|_2 = \sup_{\boldsymbol{x}\neq 0} \frac{\|QA\boldsymbol{x}\|}{\|\boldsymbol{x}\|} = \sup_{\boldsymbol{x}\neq 0} \frac{\|Q(A\boldsymbol{x})\|}{\|\boldsymbol{x}\|} = \sup_{\boldsymbol{x}\neq 0} \frac{\|A\boldsymbol{x}\|}{\|\boldsymbol{x}\|} = \|A\|_2. \qquad \square$$

LEMMA 7.3. *Let the matrix $A \in \mathbb{C}^{m\times n}$. Then $\|A^*\|_2 = \|A\|_2$.*

Proof. Let $\boldsymbol{x} \in \mathbb{C}^{n\times 1}$ be a vector such that $\boldsymbol{x} \neq 0$. Using the fact that $(A\boldsymbol{x})^*(A\boldsymbol{x}) = \boldsymbol{x}^*(A^*A\boldsymbol{x})$ and the Cauchy-Schwarz inequality, we have

$$\|A\boldsymbol{x}\|^2 \leq \|A^*A\boldsymbol{x}\|\|\boldsymbol{x}\| \leq \|A^*\|_2\|A\|_2\|\boldsymbol{x}\|^2$$

and dividing by $\|\boldsymbol{x}\|^2$ one gets

$$\frac{\|A\boldsymbol{x}\|^2}{\|\boldsymbol{x}\|^2} \leq \|A^*\|_2\|A\|_2.$$

Then

$$\sup_{\boldsymbol{x}\neq 0} \frac{\|A\boldsymbol{x}\|^2}{\|\boldsymbol{x}\|^2} \leq \|A^*\|_2\|A\|_2$$

which implies that

$$\|A\|_2^2 = \left(\sup_{\boldsymbol{x}\neq 0} \frac{\|A\boldsymbol{x}\|}{\|\boldsymbol{x}\|}\right)^2 = \sup_{\boldsymbol{x}\neq 0} \frac{\|A\boldsymbol{x}\|^2}{\|\boldsymbol{x}\|^2} \leq \|A^*\|_2\|A\|_2$$

and dividing by $\|A\|_2$ on both sides one gets

$$\|A\|_2 \leq \|A^*\|_2.$$

Similarly, $\|A^*\|_2 \leq \|(A^*)^*\|_2 = \|A\|_2$, therefore $\|A^*\|_2 = \|A\|_2$. $\square$

REFERENCES

[1] C. J. S. Alves, *On the choice of source points in the method of fundamental solutions*, Engineering Analysis with Boundary Elements, 33 (2009), pp. 1348–1361, https://doi.org/10.1016/j.enganabound.2009.05.007.
[2] C. J. S. Alves and P. R. S. Antunes, *The method of fundamental solutions applied to some inverse eigenproblems*, SIAM Journal on Scientific Computing, 35 (2013), pp. A1689–A1708, https://doi.org/10.1137/110860380.
[3] P. R. S. Antunes, *Is it possible to tune a drum?*, Journal of Computational Physics, 338 (2017), pp. 91–106, https://doi.org/10.1016/j.jcp.2017.02.056.
[4] P. R. S. Antunes, *Reducing the ill conditioning in the method of fundamental solutions*, Advances in Computational Mathematics, 44 (2018), pp. 351– 365, https://doi.org/10.1007/s10444-017-9548-6.
[5] P. R. S. Antunes, *A well-conditioned method of fundamental solutions for Laplace equation*, Numerical Algorithms, 91 (2022), pp. 1381–1405, https://doi.org/10.1007/s11075-022-01306-x.
[6] A. Araújo and P. Serranho, *On the use of quasi-equidistant source points over the sphere surface for the method of fundamental solutions*, Journal of Computational and Applied Mathematics, 359 (2019), pp. 55–68, https://doi.org/10.1016/j.cam.2019.03.019.
[7] G. B. Arfken, H. J. Weber, and F. E. Harris, *Chapter 15 - legendre functions*, in Mathematical Methods for Physicists (Seventh Edition), G. B. Arfken, H. J. Weber, and F. E. Harris, eds., Academic Press, Boston, seventh edition ed., 2013, pp. 715–772, https://doi.org/10.1016/B978-0-12-384654-9.00015-3.
[8] G. B. Arfken, H. J. Weber, and F. E. Harris, *Chapter 16 - angular momentum*, in Mathematical Methods for Physicists (Seventh Edition), G. B. Arfken, H. J. Weber, and F. E. Harris, eds., Academic Press, Boston, seventh edition ed., 2013, pp. 773–814, https://doi.org/10.1016/B978-0-12-384654-9.00016-5.
[9] O. Askour, A. Tri, B. Braikat, H. Zahrouni, and M. Potier-Ferry, *Coupling of MFS and ANM for solving nonlinear elasticity problems*, in CFM 2017 - 23ème Congrès Français de Mécanique, A. F. de Mécanique, ed., Congrès français de mécanique, Lille, France, Aug 2017, AFM, Maison de la Mécanique, 39/41 rue Louis Blanc - 92400 Courbevoie, https://hal.science/hal-03465731.
[10] J. A. Barceló, C. Castro, F. Macià, and C. J. Meroño, *The Born approximation in the three-dimensional Calderón problem*, Journal of Functional Analysis, 283 (2022), p. 109681, https://doi.org/10.1016/j.jfa.2022.109681.
[11] T. Betcke and L. N. Trefethen, *Reviving the method of particular solutions*, SIAM Rev., 47 (2005), p. 469–491, https://doi.org/10.1137/S0036144503437336.
[12] C. S. Chen, *On the determination of locating the source points of the MFS using effective condition number*, Journal of Computational and Applied Mathematics, 423 (2023), pp. 5597–5614, https://doi.org/10.1016/j.jcp.2010.03.043.
[13] C. S. Chen, H. A. Cho, and M. A. Golberg, *Some comments on the ill-conditioning of the method of fundamental solutions*, Engineering Analysis with Boundary Elements, 30 (2006), pp. 405–410, https://doi.org/10.1016/j.enganabound.2006.01.001.
[14] C. S. Chen, A. Karageorghis, and Y. Li, *On choosing the location of the sources in the MFS*, Numerical Algorithms, 72 (2016), pp. 107–130, https://doi.org/10.1007/s11075-015-0036-0.
[15] C. S. Chen, S. Reutskiy, and V. Rozov, *The method of the fundamental solutions and its modifications for electromagnetic field problems*, Computer Assisted Mechanics and Engineering Sciences, 16 (2009), pp. 21–33, https://cames.ippt.pan.pl/index.php/cames/article/view/161.
[16] A. H. Cheng and Y. Hong, *An overview of the method of fundamental solutions—solvability, uniqueness, convergence, and stability*, Engineering Analysis with Boundary Elements, 120 (2020), pp. 118–152, https://doi.org/10.1016/j.enganabound.2020.08.013.
[17] G. Feng, M. Li, and C. S. Chen, *On the ill-conditioning of the MFS for irregular boundary data with sufficient regularity*, Engineering Analysis with Boundary Elements, 41 (2014), p. 98–102, https://doi.org/10.1016/j.enganabound.2014.01.011.
[18] E. Junior, J. A. F. Santiago, and J. C. Telles, *On a regularized method of fundamental solutions coupled with the numerical Green's function procedure to solve embedded crack problems*, Engineering Analysis with Boundary Elements, 37 (2013), pp. 1 – 7, https://doi.org/10.1016/j.enganabound.2012.08.013.
[19] A. Karageorghis and D. Lesnic, *The method of fundamental solutions for the Oseen steady-state viscous flow past obstacles of known or unknown shapes*, Numerical Methods for Partial Differential Equations, 35 (2019), pp. 2103–2119, https://doi.org/10.1002/num.22404.

[20] A. Karageorghis, D. Lesnic, and L. Marin, *The method of fundamental solutions for the detection of rigid inclusions and cavities in plane linear elastic bodies*, Computers & Structures, 106-107 (2012), pp. 176–188, https://doi.org/10.1016/j.compstruc.2012.05.001.

[21] M. Katsurada, *A mathematical study of the charge simulation method ii*, J. Fac. Sci. Univ. Tokyo, Sec. IA, Math., 36 (1989), pp. 135–162, https://cir.nii.ac.jp/crid/1571980074747144704.

[22] V. D. Kupradze and M. A. Aleksidze, *The method of functional equations for the approximate solution of certain boundary value problems*, USSR Computational Mathematics and Mathematical Physics, 4 (1964), pp. 82–126, https://doi.org/https://doi.org/10.1016/0041-5553(64)90006-0.

[23] R. Mamud, N. C. Roberty, C. J. S. Alves, and N. F. M. Martins, *On the reconstruction of characteristic sources in helmholtz equations using the method of fundamental solutions.*, in Proceeding Series of the Brazilian Society of Computational and Applied Mathematics, 2017, https://doi.org/10.5540/03.2017.005.01.0492.

[24] R. G. McClarren and C. D. Hauck, *Robust and accurate filtered spherical harmonics expansions for radiative transfer*, Journal of Computational Physics, 229 (2010), pp. 5597–5614, https://doi.org/10.1016/j.jcp.2010.03.043, https://www.sciencedirect.com/science/article/pii/S0021999110001622.

[25] G. W. Stewart, *On the perturbation of pseudo-inverses, projections and linear least squares problems*, SIAM Review, 19 (1977), pp. 634–662, https://doi.org/10.1137/1019104.

[26] L. N. Trefethen and D. Bau, *Numerical Linear Algebra*, SIAM, 1997.

[27] D. L. Young, C. W. Chen, C. M. Fan, K. Murugesan, and C. C. Tsai, *The method of fundamental solutions for Stokes flow in a rectangular cavity with cylinders*, European Journal of Mechanics - B/Fluids, 24 (2005), pp. 703–716, https://doi.org/10.1016/j.euromechflu.2005.03.003.